Research Article

A Fast and Robust Approach for the Green Synthesis of Spherical Magnetite (Fe₃O₄) Nanoparticles by *Tilia tomentosa* (Ihlamur) Leaves and its Antibacterial Studies

Shashanka Rajendrachari¹* , **Abdullah Cahit Karaoglanli¹**, **Yusuf Ceylan²**, **Orhan Uzun³,⁴**

¹*Department of Metallurgical and Materials Engineering, Bartin University, Bartin-74100, Turkey.*

²*Department of Molecular Biology and Genetics, Bartın University, Bartin, Turkey.*

³*Rectorate of Bartin University, Bartin, Turkey.*

⁴*Department of Physics, Ankara University, Ankara, Turkey.*

Abstract

Background: In the past few years, Magnetite (Fe₃O₄) nanoparticles have gained a significant research interest in the field of biology, chemistry, metallurgy due to their wide range of applications. Some of their important applications include drug delivery, chemotherapy, low-friction seals, magnetic fluid, adsorbent, recovery of hazardous wastes, etc.

Methods: In the present paper, we reported an eco-friendly route of preparing magnetite nanoparticles by using leaves of *Tilia Tomentosa* (*Ihlamur*) followed by calcination at 400 ˚C for 15 minutes.

Results: The bandgap energy of the prepared Fe₃O₄ nanoparticles was studied by UV–Visible spectroscopy and the value was found to be 3.31 eV. The scanning electron microscopy (SEM) image showed the spherical magnetite nanoparticles with an average size of 25 nm. The phases and thermal properties of Fe₃O₄ nanoparticles were studied by using X-ray diffraction, thermogravimetric (TG) and differential thermal analysis (DTA). The enthalpy change of Fe₃O₄ nanoparticles was calculated by using the DTA curve and the value was found to be 4.97 kJ/mol at 8˚C/min heating rate. The antimicrobial activity of Fe₃O₄ nanoparticles was carried out by the minimum inhibition concentration (MIC) assay method. Except for *B. subtilis*, Fe₃O₄ nanoparticles demonstrated significant antibacterial property.

Conclusion: The prepared magnetite nanoparticles showed excellent thermal stability and less weight loss over a 30–1000 ˚C temperature range. The size of the prepared magnetite nanoparticles is very less therefore they interacted effectively with the organelle, enzymes, and cells of bacteria and inhibited bacterial growth by killing them.

Introduction

The world in the recent past has witnessed a very rapid development in the field of nanotechnology and its glorification in improving the living standard of people.[1] Nanotechnology has become very popular among materials scientists, chemists, biochemists, physicists, metallurgists, etc. due to its wide range of applications in various sectors.[2-5] Metal oxide nanoparticles are one of the types of nanomaterials advancing with significant velocity due to the ease of production. Compared to metal nanoparticles; metal oxide nanoparticles show extremely refined size, maximum surface area and possess excellent physical, biological, chemical, and mechanical properties.[2,3]

Recently, Fe₃O₄ nanoparticles has proved to be one of the most popular metal oxide nanoparticles due to their unique properties like superparamagnetic properties,[6] biocompatibility, pigmentation, biodegradability, non-toxic nature, etc.[7–9] All the above properties had made them to use in different applications such as catalysis (for carbon nanotube production),[10-12] magnetic storage media,[13] biosensors,[14] magnetic resonance imaging contrast agents,[15-17] targeted drug delivery,[18–20] nickel-iron batteries and as sorbents for environmental remediation.[17,21]

The Fe₃O₄ nanoparticles can be prepared by various methods like reverse micelle,[22-25] copolymer template method,[22,26,27] co-precipitation,[28] sol-gel method,[29] electrochemical method,[30] solvothermal method,[31] and hydrothermal[32] method. But the above-reported methods are sometimes tedious, slow and may require some special expensive equipment, capping agents, high temperature and templates (result in impurities), etc. Most of the

chemical methods used to prepare Fe_3O_4 nanoparticles require strong toxic reducing agents; whose by-products are very dangerous to the environment. Therefore, in the present paper, we reported a simple, rapid, inexpensive, non-toxic and eco-friendly route to prepared Fe_3O_4 nanoparticles using *Tilia tomentosa* (*Ihlamur*) plant leaves extract. Generally, the biological synthesis of metal oxide nanoparticles by plant leaves mainly depends upon solvent, pH, pressure and experimental temperature.[33] One of the major advantages of the reported method is the huge availability of biodiversity of plants; the phytochemicals like aldehydes, ketones, flavonoids and phenols present in the plant act as reducing agents and converts metal salts into metal oxide nanoparticles.[34]

Ihlamur or *Linden* grows as a tree or shrubs and belongs to the family of genus *Tilia*.[35,36] They are generally found in temperate and semi-tropical regions of the northern hemisphere. These plant leaves and flowers are used to be herbal tea for centuries in Turkey. It is a light yellowish with soothing features and proved to be very effective against the common cold, fever, headache, sore throat, high blood pressure, etc.

Moustafa et al. prepared Fe_3O_4 nanoparticles by leaves extract of *guava* for doxorubicin drug loading.[37] The shape, size, quantitative analysis was performed by using transmission electron microscopy (TEM) and UV-visible spectroscopy respectively.

Kale et al. developed an environment-friendly and cost-effective method to prepare Fe_3O_4 nanoparticles using *banana* leaves as reducing agent.[38] They reported that the protein present in banana leaves is main responsible for the reduction of ferrous sulfate into Fe_3O_4 nanoparticles.

Kanagasubbulakshmi et al. prepared Fe_3O_4 nanoparticles using *Lagenaria siceraria* leaves extract. Most of the leaves extract acts as a reducing agent due to the presence of phytochemicals. They reported that the magnetite nanoparticles exhibits excellent antioxidant property and excellent hydrophilic nature due to the presence of functional groups like –OH and –COOH. They also studied the antimicrobial property of magnetite nanoparticles successfully against Gram-negative - *Escherichia coli*, Gram-positive- *Staphylococcus aureus*.[39]

Generally, capping agents are used to reduce particle agglomeration in the case of physical and chemical methods of preparing nanoparticles, but our proposed green synthesis method does not require toxic and expensive capping agents separately. The phytochemicals present in *Ihlamur* leaves itself acts as a reducing agent as well as capping agent. Therefore, we aimed to develop low cost, robust, nontoxic and eco-friendly processes to synthesis nanoparticles and the proposed method satisfies the mentioned requirements successfully.

Kivrak et al. reported a detail investigation of the phenolic composition of *Tilia tomentosa* leaves in their previous publication.[40] Many of the researchers have already published a green synthesis of magnetite nanoparticles, but no literature is available on the green synthesis of magnetite nanoparticles using *Ihlamur* plant leaves. Therefore, in the present paper, we reported the preparation of Fe_3O_4 nanoparticles by using *Ihlamur* leaves and studied their antibacterial activities.

Materials and Methods
Chemicals and reagents required
Iron (III) chloride hexahydrate [$FeCl_3.6H_2O$], Iron (II) chloride tetrahydrate [$FeCl_2.4H_2O$], sodium hydroxide (NaOH) of Sigma-Aldrich brand was purchased from Umay laboratuvar, Istanbul, Turkey. *Tilia tomentosa* (*Ihlamur*) plant extract was prepared in the lab and all the solutions were prepared by using double distilled water.

Preparation of plant extract
The dried leaves of *Tilia tomentosa* (*Ihlamur*) were collected from the market of Bartin, Turkey with the help of an expert from Bartin University, Turkey and were pulverized using a blender to get uniform powders. Five grams of powdered leaves of *Ihlamur* were mixed with 100 mL of deionized water and the solution was boiled around 80 ˚C for 15 to 20 minutes until we get a strong yellow colored solution. Then the solution was cooled to room temperature (around 25 ˚C) and filtered through general-purpose filter papers followed by centrifugation to get a clear yellow colored solution of plant extract. This plant extract acts as both reducing agents as well as capping agents in preparing Fe_3O_4 nanoparticles due to the presence of phenolic compounds like caffeic, p-coumaric, chlorogenic acids, etc. and flavonoids like quercetin glycosides, kaempferol glycosides, tyliroside, etc.[40] A small amount of the extract was used all the time during the experiment to prepare magnetite nanoparticles and remaining aliquots of plant extract was stored at 5 ˚C temperature for further use. Figure 1 shows the *Tilia tomentosa* (*Ihlamur*) leaves, its extract and colloidal solution of Fe_3O_4 nanoparticles.

Preparation of Fe_3O_4 nanoparticles
One gram of Iron (III) Chloride Hexahydrate and two grams of Iron (II) Chloride Tetrahydrate powders were dissolved in 100 mL of deionized water. Then the solution was stirred on a magnetic stirrer for 10 minutes at 80 ˚C to get a homogeneous solution. Later added 10 mL of *Ihlamur* plant extract slowly to get dark brownish color indicating the initial generation of magnetite nanoparticles and the solution was stirred at 80 ˚C for 10 minutes on a magnetic stirrer. Then 0.1 M NaOH was added dropwise to precipitate out all the brownish color solution as a black colored solution. Stir the solution for 10 minutes more at 80 ˚C for the complete precipitation of magnetite nanoparticles and then cooled to room temperature.

The obtained solution was further centrifuged for 10 minutes at 7500 rpm to remove all the impurities by removing the supernatant solution. Then the nanoparticles were washed again by water and centrifuged at least 3 times. Fe_3O_4 nanoparticles were collected on a watch glass and dried at 70 ˚C in a laboratory oven overnight.
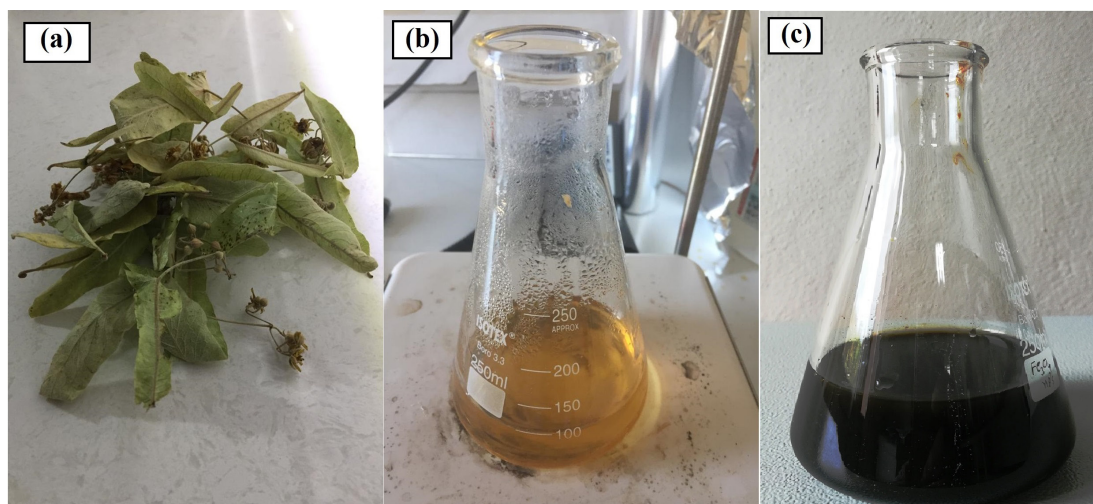
Figure 1. (a) *Tilia tomentosa* (*Ihlamur*) leaves and **(b)** *Ihlamur* leaves extract **(c)** Colloidal solution of Fe₃O₄ nanoparticles.
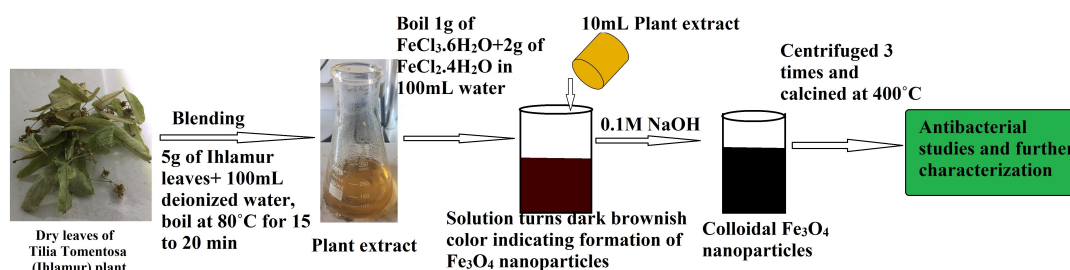

Figure 2. Schematic representation of the preparation of Fe₃O₄ nanoparticles.

The dried dark brown colored Fe_3O_4 nanoparticles were further calcined in a furnace at 400 ˚C with a holding time of 15 minutes to remove any evaporable impurities. The calcined samples were cooled to room temperature, pulverized and then stored for further characterization. Figure 2 shows the schematic representation of preparing Fe_3O_4 nanoparticles.

Characterization of Fe₃O₄ nanoparticles

XRD (RIGAKU SmartLab) was used to study the phases of prepared Fe_3O_4 nanoparticles with the 2θ range between 20-80˚ using Cu Ka$_{a1}$ radiation (λ=1.54056 Å). The morphology of the nanoparticles was investigated by using SEM (TESCAN- MAIA3 XMU) and their quantitative analysis was carried out by using energy dispersive spectroscopy (EDS) attached to SEM. UV-Visible spectroscopy (Shimadzu- UV 3600 Plus) was used to study the optical properties of magnetite nanoparticles respectively. Hitachi, STA 7300 model was used to study the thermal properties. Antibacterial activities of the prepared magnetite (Fe_3O_4) nanoparticles were studied by using gram-negative and gram-positive bacteria by the MIC assay method.

Antibacterial activity

The antibacterial properties of green synthesized Fe_3O_4 nanoparticles were investigated against three gram (+) (*Bacillus subtilis, Enterococcus faecalis, Staphylococcus aureus*) and three gram-negative bacteria (*Escherichia*

coli, Salmonella enteritidis, Pseudomonas aeruginosa) respectively. All the tested bacteria were provided by the Department of Molecular Biology and Genetic of Bartin University (Bartin, Turkey). Andrews et al.[41] reported the MIC that inhibits bacterial growth under normal conditions. All bacteria were inoculated to *Luria Bertani* broth and bacterial growths were standardized to 0.5 McFarland standard turbidity (1.5x108 CFU/ml). The same volume of growth medium and solution were added into the first well of 96 well plates, and the mixture was diluted from 50 mM to 1.5625 mM using a 96-well microplate that was incubated at 37 ˚C.

The MIC value was determined according to the turbidity of bacterial growth by the UV-Visible spectrum at 600 nm. The suspended wells were inoculated into Petri dishes that contained Mueller Hinton Agar and were incubated at 37 ˚C for 24 h. MIC is the lowest concentration required to inhibit bacterial growth. Minimum Bactericidal Concentration (MBC) assay determines the lowest concentration required to kill microorganisms.

Results and discussion
X-Ray diffraction

XRD diffraction pattern of Fe_3O_4 nanoparticles prepared by *Tilia tomentosa* (*Ihlamur*) leaves extract is shown in Figure 3. The diffraction peaks at 2θ of 30.08°, 35.46° and 43.19° corresponds to (220), (311) and (400) planes respectively and all the diffraction peaks were perfectly matched with the JCPDF Card No.: 00-001-1111. According to the The
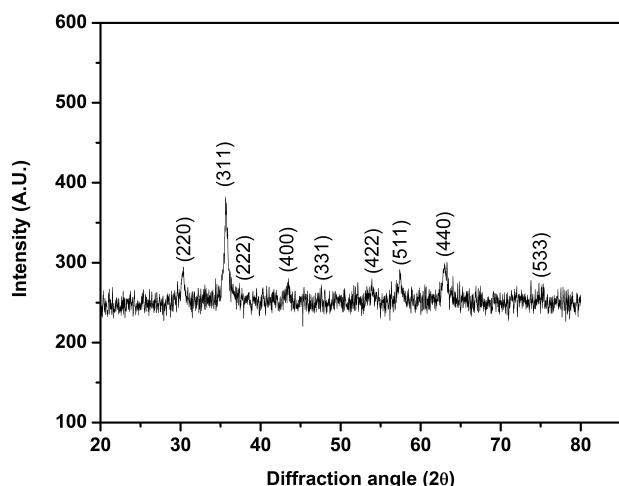
Figure 3. XRD diffraction spectra of Fe$_3$O$_4$ nanoparticles prepared by using *Tilia Tomentosa* (*Ihlamur*) leaves extract.

XRD data, the diffraction peaks of prepared magnetite nanoparticles are short and broadened and exhibited a single-phase cubic structure with space group Fd-3m(227). XRD data, the diffraction peaks of prepared magnetite nanoparticles are short and broadened and exhibited a single-phase cubic structure with space group Fd-3m (227) crystallite size of prepared magnetite nanoparticles were calculated by Scherrer's formula[42,43] as follows:

$$D = \frac{K\lambda}{\beta \cos \theta}$$

Eq. (1)

Where, D= Average crystallite size, K= A constant equal to 0.94, λ= the wavelength of X-ray radiation (0.154 nm), β= Full-width half maximum of the peak (FWHM) (in radians) and 2θ= Bragg's angle (degree). We have calculated the crystallite size for the 2 high-intensity peaks (311) and (440) using Scherrer's equation and the values were found to be ≈15 nm and ≈13 nm respectively.

Aparna et al. reported that, as the crystallite size of the particles decreases to below 20 nm they will show maximum lattice strain than the particles with more than 20 nm crystallite size.[44] Therefore, our magnetite nanoparticles are expected to have maximum strain due to

the refined size of almost 15 nm (Scherrer's calculations). Therefore, we have decided to calculate the lattice strain by using Williamson-Hall equation[45,46] as follows:

$$\beta cos\theta = \frac{0.94\lambda}{D} + 4\varepsilon \, sin\theta$$

Eq. (2)

Where 'β' is FWHM, 'ε' is the strain, 'D' is the average crystallite size and 'θ' is the Bragg's diffraction angle. Williamson and Hall proposed a method for de-convoluting the size and strain broadening by looking at the peak width as a function of 2θ.[47-50] The average crystallite size and lattice strain of prepared of magnetite nanoparticles were calculated by Williamson-Hall equation and were found to be ~9 nm and 0.41 respectively. Broadening of the diffraction peaks is generally due to the reduced crystallite size, instrumental errors and lattice strain.[51-53]

Scanning electron microscopy

The SEM analysis of the prepared Fe$_3$O$_4$ nanoparticles is shown in Figure 4 (a). If we observe the SEM images carefully one can see the cubic and averagely spherical magnetite nanoparticles with almost the same dimensions. The average particle size of prepared magnetite nanoparticles was found to be around 20 nm. Generally, capping agents are used to reduce agglomeration, but we did not use any such capping agents due to their toxic nature and are very expensive. The plant extract itself acts as both reducing agent as well as capping agent; therefore the prepared nanoparticles are homogeneous with little or no agglomeration. Therefore, this method is very much environmentally friendly and cost-effective.

We also performed EDS to study the elemental composition present in prepared magnetite nanoparticles in detail. Figure 4 (b) depicts the EDS image of Fe$_3$O$_4$ nanoparticles prepared by *Ihlamur* plant extract. The atomic percentage of iron and oxygen was theoretically calculated as 50% each. Similarly, the experimental atomic percentage of copper and oxygen were found to be 50% each. Both iron and oxygen atoms present in prepared Fe$_3$O$_4$ nanoparticles are stoichiometric to each other and agree with the theoretical values.
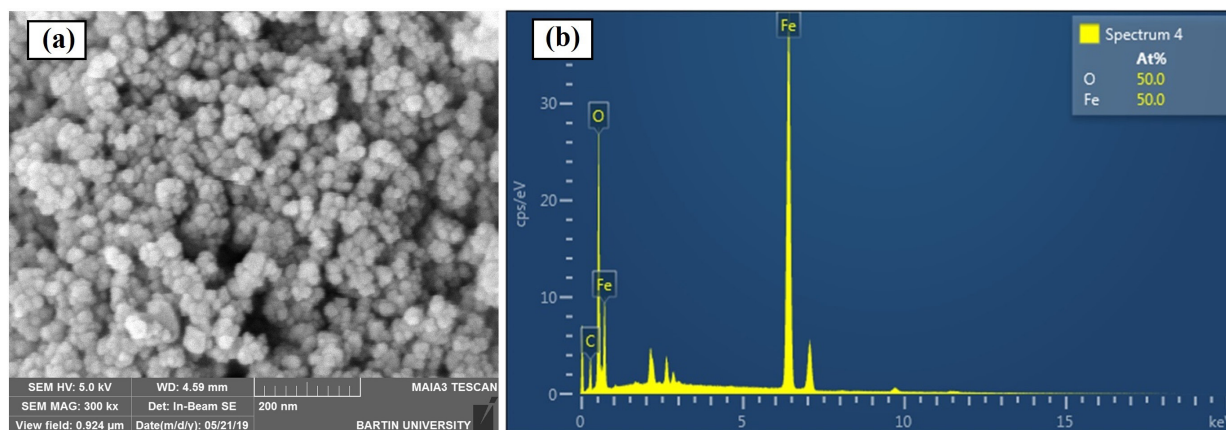
Figure 4. (a) SEM image of Fe$_3$O$_4$ nanoparticles **(b)** Energy dispersed spectroscopy (EDS) image of Fe$_3$O$_4$ nanoparticles prepared by *Ihlamur* plant leaves.
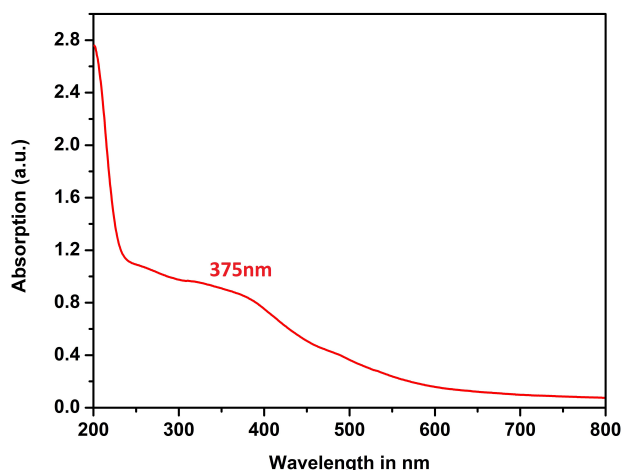
Figure 5. UV-Visible spectra of green synthesized Fe$_3$O$_4$ nanoparticles.

Figure 6. TG and DTA curve of green synthesized Fe$_3$O$_4$ nanoparticles at 8˚C/minute heating rate.

UV-Visible spectroscopy

Figure 5 represents the UV-Visible spectra of Fe$_3$O$_4$ nanoparticles prepared from *Ihlamur* leaves. The prepared nanoparticles were dispersed in de-ionized water using an ultra sonicator for 2 minutes to get a homogeneous solution. Generally, UV-Visible spectroscopy uses light in the near-UV and near-infrared ranges and in this visible range molecules undergo electronic transitions and directly nanoparticles prepared from Ihlamur leaves. The prepared nanoparticles were dispersed in de-ionized water using an ultra sonicator for 2 minutes to get a homogeneous solution. Generally, UV-Visible spectroscopy uses light in the near-UV and near-infrared ranges and in this visible range molecules undergo electronic transitions and directly affect the perceived color of the chemicals involved.[37]

The UV-Visible spectrum shows a broad surface Plasmon resonance absorption peak at 375 nm.

This surface plasmon resonance absorption phenomenon occurs due to the collective oscillation of the free conduction band electrons when electromagnetic radiation strikes them and incident light far exceeds the particle diameter.[54] The bandgap energy (E) of the prepared magnetite nanoparticles were calculated by using the following equation,[55]

$$E = \frac{h \times C}{\lambda}$$

Eq. (3)

Where E = Bandgap energy
  h = Planks constant = 6.626×10^{-34} Joules.sec
  C = Speed of light = 3.0×10^8 meter/sec
  λ = Cut off wavelength = 375×10^{-9} meters
  *Conversion 1eV=1.6×10^{-19} Joules

The calculated band gap energy of magnetite nanoparticles was found to be 3.31 eV. H.El Ghandoor et al.[56] reported the bandgap of magnetite nanoparticles as 3.64 eV, and Fouad El-Diasty et al.[57] reported the same as 5.7 eV. Our calculated band gap values are less than reported values and this confirms that our sample is more conductive than theirs.[56,57]
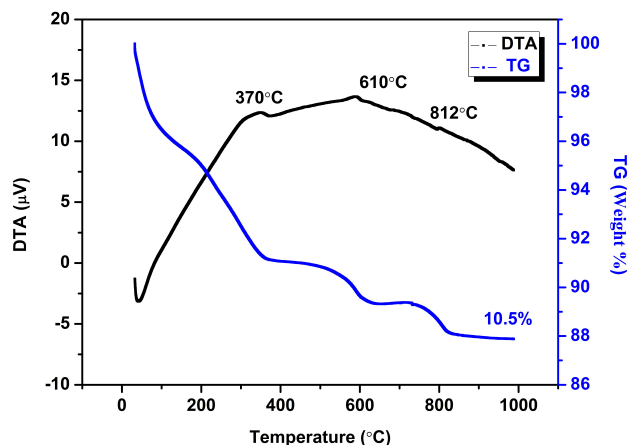
Thermal analysis

Thermogravimetric analysis (TG) and differential thermal analysis (DTA) was carried out to study the thermal properties of prepared Fe$_3$O$_4$ nanoparticles over a temperature range of 30–1000 ˚C. Figure 6 represents the TG and DTA curve of Fe$_3$O$_4$ nanoparticles at 8 ˚C/minute heating rate.

Synthesized magnetite nanoparticles showed excellent thermal stability and very less weight loss over a 30–1000 ˚C temperature range. This is due to the significant resistance of magnetite nanoparticles against evaporation and phase change at that temperature range. Only 4.1% weight loss was observed between 30 to 120 ˚C due to water evaporation and nearly 4.9% weight loss was observed at 120–370 ˚C due to the decomposition of thermal properties of prepared Fe3O4 nanoparticles over a temperature range of 30–1000 ˚C. Figure 6 represents the TG and DTA curve of Fe3O4 nanoparticles at 8 ˚C/minute heating rate.

Synthesized magnetite nanoparticles showed excellent thermal stability and very less weight loss over a 30–1000 ˚C temperature range. This is due to the significant resistance of magnetite nanoparticles against evaporation and phase change at that temperature range. Only 4.1% weight loss was observed between 30 to 120 ˚C due to water evaporation and nearly 4.9% weight loss was observed at 120–370 ˚C due to the decomposition of organic material and carbonaceous matter.[58] From the graph, one can observe 1.5% weight loss around 610 ˚C due to the phase transformation from Fe$_3$O$_4$ to FeO, as FeO is thermodynamically more stable above 570 ˚C according to the Fe-O phase diagram.[59]

At higher temperatures there is a possibility of deoxidation of FeO under the N$_2$ atmosphere as reported by S.Y Zhao et al.[60] The total weight loss over a temperature range of 30–1000 ˚C was found to be 10.5%.

Synthesized magnetite nanoparticles showed excellent thermal stability and very less weight loss over a 30–1000 ˚C temperature range. This is due to the significant resistance of magnetite nanoparticles against evaporation and phase change at that temperature range. Only 4.1%
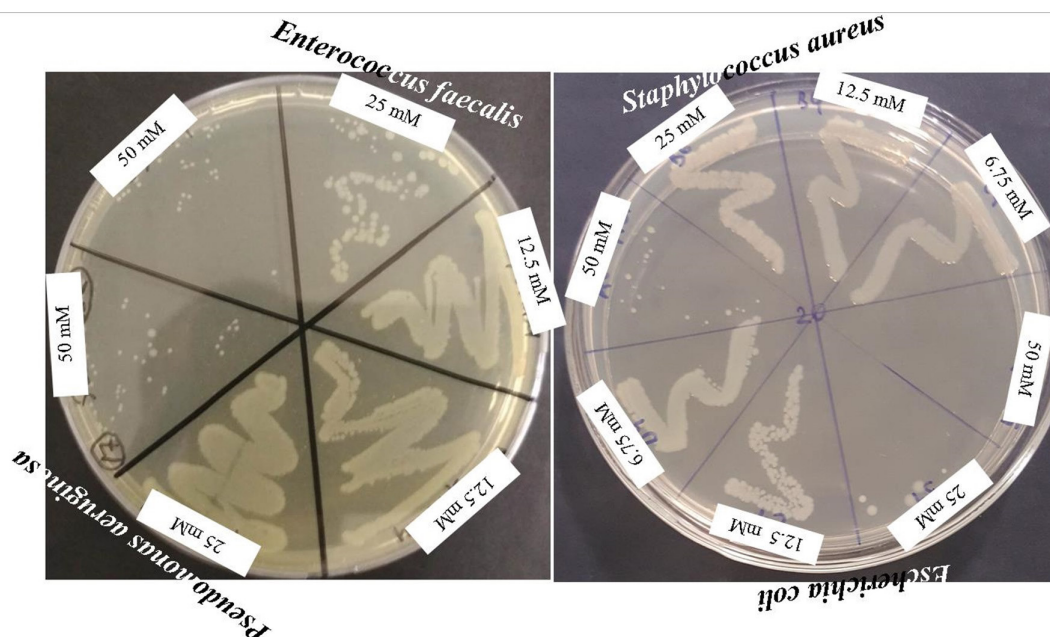
Figure 7. The MIC and MBC results of Fe₃O₄ nanoparticles against bacterial strains.

weight loss was observed between 30 to 120 ˚C due to water evaporation and nearly 4.9% weight loss was observed at 120–370 ˚C due to the decomposition of organic material and carbonaceous matter.[58] From the graph, one can observe 1.5% weight loss around 610 ˚C due to the phase transformation from Fe_3O_4 to FeO, as FeO is thermodynamically more stable above 570 ˚C according to the Fe-O phase diagram.[59] At higher temperatures there is a possibility of deoxidation of FeO under the N_2 atmosphere as reported by S.Y Zhao et al.[60] The total weight loss over a temperature range of 30–1000 ˚C was found to be 10.5%.

According to DTA curves at 8 ˚C/min heating rate, we can observe endothermic peaks at 370, 610 and 812 ˚C respectively. These endothermic peaks confirm the decomposition of organic matter and carbonaceous materials, the phase transformation from Fe_3O_4 to FeO, and the deoxidation of FeO, respectively. The enthalpy change of prepared magnetite nanoparticles at 8 ˚C/min was found to be 4.97 kJ/mol.

Antibacterial activity

The antibacterial effect of Fe_3O_4 nanoparticles was tested against six bacteria strains namely *Bacillus subtilis, Enterococcus faecalis, Escherichia coli, Pseudomonas aeruginosa, Salmonella enteritidis, Staphylococcus aureus.* Except for *B. subtilis*, Fe_3O_4 nanoparticles demonstrated excellent antibacterial property. The Fe_3O_4 nanoparticles at 25 mM and 50 mM was respectively demonstrated MIC property against *E. faecalis, S. enteritidis, E. coli* and *P. aeruginosa, S. aureus*; but it show MBC against *E. coli* only at 50 mM. Figure 7 depicts the antibacterial effect of prepared magnetite nanoparticles.

Arokiyaraj et al.[61] have studied the antibacterial effect of iron oxide nanoparticles prepared from the leaves of *Argemone mexicana* against *E. coli, Proteus mirabilis*, and

B. subtilis by disc diffusion method. According to their result, the iron oxide showed an inhibitory effect and formed zones against three bacteria. Groiss et al.[62] have reported that the iron oxide obtained from *Cynometra ramiflora* leaf extract is very effective in inhibiting *E. coli and S. epidermidis* and may find its application in the antibacterial drug development.

The size of prepared magnetite nanoparticles is very much suitable for cell permeability. They can interact effectively with the organelle, enzymes, and cells of bacteria and inhibits bacterial growth by killing them, deactivating the enzymes, tearing the cell wall of bacteria or by cutting the body of bacteria.[63] Hence, the prepared Fe_3O_4 nanoparticles were found to be a significant antibacterial material that demonstrates an excellent lethal activity against tested bacteria. The obtained results depict the possible use of prepared magnetite nanoparticles as a promising tool for improved therapeutic efficacy and diagnostic applications in the medical field.

Conclusion

In this project, we could successfully prepared Fe_3O_4 nanoparticles by an easy and eco-friendly plant-mediated biological method using leaves of *Tilia tomentosa* (*Ihlamur*). The prepared magnetite nanoparticles showed a single-phase cubic structure with an average crystallite size of 9 nm and a lattice strain of 0.41 as calculated from the Williamson-Hall equation. SEM studies revealed the spherical nature of the prepared nanoparticles with less agglomeration. The EDS analysis confirmed the 50:50 stoichiometric ratios of iron and oxygen theoretically and experimentally. UV-Visible spectroscopy of magnetite nanoparticles showed a broad surface Plasmon resonance absorption peak at 375 nm. The prepared iron oxide nanoparticles exhibited a bandgap of 3.31 eV and which

was quite less compared to other reported values and hence more conductive. The enthalpy change of prepared nanoparticles is calculated by using a DTA curve and the value was found to be 4.97 kJ/mol at 8 ˚C/min heating rate. We also successfully investigated the antibacterial activity of the prepared magnetite nanoparticles against *Bacillus subtilis, Enterococcus faecalis, Escherichia coli, Pseudomonas aeruginosa, Salmonella enteritidis, Staphylococcus aureus*. Except for *B. subtilis*, Fe_3O_4 nanoparticles demonstrated excellent antibacterial property.

Conflict of Interests
The authors declare that there are no conflicts of interest.

References
1. Yew YP, Shameli K, Miyake M, Kuwano N, Bt Ahmad Khairudin NB, Bt Mohamad SE, et al. Green Synthesis of Magnetite (Fe_3O_4) Nanoparticles Using Seaweed (*Kappaphycus alvarezii*) Extract. Nanoscale Res Lett. 2016;11(1):276. doi:10.1186/s11671-016-1498-2

2. Noguera C. Physics and Chemistry at Oxide Surfaces. Cambridge, UK: Cambridge University Press; 1996.

3. Kung HH. Transition Metal Oxides: Surface Chemistry and Catalysis. Amsterdam: Elsevier; 1989.

4. Henrich VE, Cox PA. The Surface Chemistry of Metal Oxides. Cambridge, UK: Cambridge University Press; 1994.

5. Shashanka R. Non-lubricated dry sliding wear behavior of spark plasma sintered nano-structured stainless steel. J Mater Environ Sci . 2019;10(8):767-77.

6. Mahdavian AR, Mirrahimi MAS. Efficient separation of heavy metal cations by anchoring polyacrylic acid on superparamagnetic magnetite nanoparticles through surface modification. Chem Eng J. 2010;159(1-3):264–71. doi:10.1016/j.cej.2010.02.041

7. Hu FQ, Wei L, Zhou Z, Ran YL, Li Z, Gao MY. Preparation of biocompatible magnetite nanocrystals for in vivo magnetic resonance detection of cancer. Adv Mater. 2006;18(19):2553-6. doi:10.1002/adma.200600385

8. Zhao H, Saatchi K, Häfeli UO. Preparation of biodegradable magnetic microspheres with poly(lactic acid)-coated magnetite. J Magn Magn Mater. 2009;321(10):1356-63. doi:10.1016/j.jmmm.2009.02.038

9. Zhang L, Dong WF, Sun HB. Multifunctional superparamagnetic iron oxide nanoparticles: design, synthesis and biomedical photonic applications. Nanoscale. 2013;5(17):7664-84. doi:10.1039/c3nr01616a

10. Gawande MB, Branco PS, Varma RS. Nano-magnetite (Fe_3O_4) as a support for recyclable catalysts in the development of sustainable methodologies. Chem Soc Rev. 2013;42(8):3371-93. doi:10.1039/C3CS35480F

11. Shelke SN, Bankar SR, Mhaske GR, Kadam SS, Murade DK, Bhorkade SB, et al. Iron oxide-supported copper oxide nanoparticles (nanocat-Fe-CuO): magnetically recyclable catalysts for the synthesis of pyrazole derivatives, 4-methoxyaniline, and ullmann-type condensation reactions. ACS Sustainable Chem Eng. 2014;2(7):1699-706. doi:10.1021/sc500160f

12. Wong EW, Bronikowski MJ, Hoenk ME, Kowalczyk RS, Hunt BD. Submicron Patterning of Iron Nanoparticle Monolayers for Carbon Nanotube Growth. Chem Mater. 2005;17(2):237-41. doi:10.1021/cm048795m

13. Terris BD, Thomson T. Nanofabricated and self-assembled magnetic structures as data storage media. J Phys D Appl Phys. 2005;38(12):R199-R222. doi:10.1088/0022-3727/38/12/R01

14. Kavitha AL, Prabu HG, Babu SA, Suja SK. Magnetite nanoparticles chitosan composite containing carbon paste electrode for glucose biosensor application. J Nanosci Nanotechnol. 2013;13(1):98-104. doi:0.1166/jnn.2013.6720

15. Chaki SH, Malek TJ, Chaudhary MD, Tailor JP, Deshpande MP. Magnetite Fe_3O_4 nanoparticles synthesis by wet chemical reduction and their characterization. Adv Nat Scinanosci. 2015;6(3):035009. doi:10.1088/2043-6262/6/3/035009

16. Jun W, Huh M, Choi S, Lee H, Song T, Kim S, et al. Nanoscale size effect of magnetic nanocrystals and their utilization for cancer diagnosis via magnetic resonance imaging. J Am Chem Soc. 2005;127(16):5732-3. doi:10.1021/ja0422155

17. Li F, Vipulanandan C, Mohanty KK. Microemulsion and solution approaches to nanoparticle iron production for degradation of trichloroethylene. Colloids Surf A Physicochem Eng Asp. 2003;223(1-3):103-12. doi:10.1016/S0927-7757(03)00187-0

18. Salem M, Xia Y, Allan A, Rohani S, Gillies ER. Curcumin-loaded, folic acid-functionalized magnetite particles for targeted drug delivery. RSC Adv. 2015;5(47):37521-32. doi:10.1039/c5ra01811k

19. Li X, Li H, Liu G, Deng Z, Wu S, Li P, et al. Magnetite-loaded fluorine-containing polymeric micelles for magnetic resonance imaging and drug delivery. Biomaterials. 2012;33(10):3013-24. doi:10.1016/j.biomaterials.2011.12.042

20. Wani KD, Kadu BS, Mansara P, Gupta P, Deore AV, Chikate RC, et al. Synthesis, characterization and in vitro study of biocompatible cinnamaldehyde functionalized magnetite nanoparticles (CPGF Nps) for hyperthermia and drug delivery applications in breast cancer. PLoS One. 2014;9(9):e107315. doi:10.1371/journal.pone.0107315

21. Zhang WX. Nanoscale Iron Particles for Environmental Remediation: An Overview. J Nanopart Res. 2003;5(3-4):323-32.

22. Blaney L. Magnetite (Fe$_3$O$_4$): Properties, Synthesis, and Applications. Lehigh Rev . 2007;15:33-81.

23. Fried T, Shemer G, Markovich G. Ordered two dimensional arrays of ferrite nanoparticles. Adv Mater. 2001;13(15):1158-61. doi:10.1002/1521-4095(200108)13:15<1158::aid-adma1158>3.0.co;2-6

24. Tang J, Myers M, Bosnick KA, Brus LE. Magnetite Fe$_3$O$_4$ nanocrystals: spectroscopic observation of aqueous oxidation kinetics. J Phys Chem B. 2003;107(30):7501-6. doi:10.1021/jp027048e

25. Zhou ZH, Wang J, Liu X, Chan HSO. Synthesis of Fe$_3$O$_4$ nanoparticles from emulsions. J Mater Chem. 2001;11(6):1704-9. doi:10.1039/B100758K

26. Breulmann M, Colfen H, Hentze HP, Antonietti M, Walsh D, Mann S. Elastic magnets: template-controlled mineralization of iron oxide colloids in a sponge-like gel matrix. Adv Mater. 1998;10(3):237-41. doi:10.1002/(sici)1521-4095(199802)10:3<237::aid-adma237>3.0.co;2-6

27. Morais PC, Garg VK, Oliveira AC, Azevedo RB, Rabelo D, Lima ECD. Synthesis and characterization of magnetite nanoparticles embedded in copolymer microspheres. Eur Cell Mater. 2002;3:173-5.

28. Venkatesan M, Nawka S, Pillai SC, Coey JMD. Enhanced magnetoresistance in nanocrystalline magnetite. Appl Phys. 2003;93(10):8023-5. doi:10.1063/1.1555371

29. Xu J, Yang H, Fu W, Du K, Sui Y, Chen J, et al. Preparation and magnetic properties of magnetite nanoparticles by sol–gel method. J Magn Magn Mater. 2007;309(2):307-11. doi:10.1016/j.jmmm.2006.07.037

30. Cabrera L, Gutierrez S, Menendez N, Morales P, Herrasti P. Magnetite nanoparticles: Electrochemical synthesis and characterization. Electrochim Acta. 2008;53(8):3436-41. doi:10.1016/j.electacta.2007.12.006

31. Liu XM, Kim JK. Solvothermal synthesis and magnetic properties of magnetite nanoplatelets. Mater Lett. 2009;63(3-4):428-30. doi:10.1016/j.matlet.2008.11.001

32. Zhang ZJ, Chen XY, Wang BN, Shi CW. Hydrothermal synthesis and self-assembly of magnetite (Fe$_3$O$_4$) nanoparticles with the magnetic and electrochemical properties. J Cryst Growth. 2008;310(24):5453-57. doi:10.1016/j.jcrysgro.2008.08.064

33. Singh J, Dutta T, Kim KH, Rawat M, Samddar P, Kumar P. 'Green' synthesis of metals and their oxide nanoparticles: applications for environmental remediation. J Nanobiotechnology. 2018;16(84):84. doi:10.1186/s12951-018-0408-4

34. Doble M, Kruthiventi AK. Green chemistry and engineering. 1st ed. Academic Press; 2007.

35. McCarthy D. Systematics and Phylogeography of the Genus *Tilia* in North America [dissertation]. Chicago: University of Illinois; 2012.

36. Wikipedia, Linden. https://tr.wikipedia.org/wiki/*Ihlamur*. Accessed May 2019.

37. Moustafa MH, Al Din RS. Green synthesis and characterization of iron-oxide nanoparticles by *guava* aqueous leaves extract for doxorubicin drug loading. J Biosci Appl Res. 2017;3(1):177-80.

38. Kale RD, Barwar S, Kane P, Bhatt L. Green Synthesis of Magnetite Nanoparticles using *Banana* Leaves. European Journal of Sciences (EJS). 2018;1(1):26-34. doi:10.29198/ejs1803

39. Kanagasubbulakshmi S, Kadirvelu K. Green synthesis of iron oxide nanoparticles using *lagenaria siceraria* and evaluation of its antimicrobial activity. Def Life Sci J. 2017;2(4):422-7. doi:10.14429/dlsj.2.12277

40. Kivrak S, Göktürk T, Kivrak I. Determination of Phenolic Composition of *Tilia tomentosa* Flowers Using UPLC-ESI-MS/MS. Int J Second Metab. 2017;4(3):249-56. doi:10.21448/ijsm.371721

41. Andrews JM. Determination of minimum inhibitory concentrations. J Antimicrob Chemother. 2002;49(6):1049. doi:10.1093/jac/dkf083

42. Shashanka R, Chaira D. Phase transformation and microstructure study of nano-structured austenitic and ferritic stainless steel powders prepared by planetary milling. Powder Technol. 2014;259:125-36. doi:10.1016/j.powtec.2014.03.061

43. Reddy S, Swamy BEK, Aruna S, Kumar M, Shashanka R, Jayadevappa H. Preparation of NiO/ZnO hybrid nanoparticles for electrochemical sensing of dopamine and uric acid. Chem Sens. 2012;2:1-7.

44. Aparna Y, Rao VK, Subbarao PS. Preparation and Characterization of CuO Nanoparticles by Novel Sol-Gel Technique. J Nano-Electron Phys. 2012;4(3):03005.

45. Shashanka R, Chaira D. Optimization of milling parameters for the synthesis of nano-structured duplex and ferritic stainless steel powders by high energy planetary milling. Powder Technol. 2015;278:35-45. doi:10.1016/j.powtec.2015.03.007

46. Shashanka R, Chaira D. Development of nano-structured duplex and ferritic stainless steel by pulverisette planetary milling followed by pressureless sintering. Mater Charact. 2015;99:220-9. doi:10.1016/j.matchar.2014.11.030

47. Shashanka R. Effect of Sintering Temperature on the Pitting Corrosion of Ball Milled Duplex Stainless Steel by using Linear Sweep Voltammetry. Anal Bioanal Electrochem. 2018;10(3):349-61.

48. Shashanka R, Chaira D, Swamy BEK. Electrocatalytic Response of Duplex and Yittria Dispersed Duplex Stainless Steel Modified Carbon Paste Electrode in Detecting Folic Acid Using Cyclic Voltammetry. Int J Electrochem Sci. 2015;10(7):5586-98.

49. Nayak AK, Shashanka R, Chaira D. Effect of Nanosize Yittria and Tungsten Addition to Duplex Stainless Steel During High Energy Planetary Milling. IOP Conf Ser Mater Sci Eng. 2016;115:012008. doi:10.1088/1757-899X/115/1/012008

50. Gupta S, Shashanka R, Chaira D. Synthesis of nano-structured duplex and ferritic stainless steel powders by planetary milling: An experimental and simulation study. IOP Conf Ser Mater Sci Eng. 2015;75:012033.

doi:10.1088/1757-899X/75/1/012033

51. Shashanka R, Swamy BEK, Sathish R, Chaira D. Synthesis of Silver Nanoparticles and their Applications. Anal Bioanal Electrochem. 2013;5(4):455-66.

52. Shashanka R, Chaira D. Effect of Y_2O_3 nanoparticles on corrosion study of spark plasma sintered duplex and ferritic Stainless steel samples by linear sweep voltammetric method. Arch Metall Mater. 2018;63(2):749-63.

53. Shashanka R. Investigation of Electrochemical Pitting Corrosion by Linear Sweep Voltammetry: A Fast and Robust Approach. In: Nobanathi Wendy Maxakato, Sandile Surprise Gwebu, Gugu Hlengiwe Mhlongo editors. Voltammetry. UK: Intechopen; 2019. p. 77-90.

54. Dhaneswar D, Nath BC, Phukon P, Doluia SK. Synthesis and evaluation of antioxidant and antibacterial behavior of CuO nanoparticles. Colloids Surf B Biointerfaces. 2013;101:430-3. doi:10.1016/j.colsurfb.2012.07.002

55. Dharma J, Pisal A. Application Note, UV/Vis/NIR Spectrometer. PerkinElmer, Inc. 940 Winter Street, Waltham. MA 02451. USA.

56. El Ghandoor H, Zidan HM, Khalil MMH, Ismail MIM. Synthesis and Some Physical Properties of Magnetite (Fe_3O_4) Nanoparticles. Int J Electrochem Sci. 2012;7(6):5734-45.

57. El-Diasty F, El-Sayed HM, El-Hosiny FI, Ismail MIM. Complex susceptibility analysis of magneto-fluids: Optical band gap and surface studies on the nanomagnetite-based particles. Curr Opin Solid State Mater Sci. 2009;13(1-2):28-34. doi:10.1016/j.cossms.2008.09.002

58. Salunkhe AB, Khot VM, Ruso JM, Patil SI. Synthesis and magnetostructural studies of amine functionalized superparamagnetic iron oxide nanoparticles. RSC Adv. 2015;5(24):18420-8. doi:10.1039/c5ra00049a

59. Mahdavi M, Ahmad MB, Haron MJ, Namvar F, Nadi B, Ab Rahman MZ, et al. Synthesis, Surface Modification and Characterisation of Biocompatible Magnetic Iron Oxide Nanoparticles for Biomedical Applications. Molecules. 2013;18(7):7533-48. doi:10.3390/molecules18077533

60. Zhao SY, Lee DG, Kim CW, Cha HG, Kim YH, Kang YS. Synthesis of magnetic nanoparticles of Fe_3O_4 and $CoFe_2O_4$ and their surface modification by surfactant adsorption. Bull Korean Chem Soc. 2006;27(2):237-42. doi:10.5012/bkcs.2006.27.2.237

61. Arokiyaraj S, Saravanan M, Prakash NKU, Arasu MV, Vijayakumar B, Vincent S. Enhanced antibacterial activity of iron oxide magnetic nanoparticles treated with *Argemone mexicana* L. leaf extract: An in vitro study. Mater Res Bull. 2013;48(9):3323-7. doi:10.1016/j.materresbull.2013.05.059

62. Groiss S, Selvaraj R, Varadavenkatesan T, Vinayagam R. Structural characterization, antibacterial and catalytic effect of iron oxide nanoparticles synthesised using the leaf extract of *Cynometra ramiflora*. J Mol Struct. 2017;1128:572-8. doi:10.1016/j.molstruc.2016.09.031

63. Rajendrachari S, Kamaci Y, Taş R, Ceylan Y, Bülbül AS, Uzun O, et al. Antimicrobial Investigation of CuO and ZnO Nanoparticles Prepared by a Rapid Combustion Method. Phys Chem Res. 2019;7(4):799-812. doi:10.22036/pcr.2019.199338.1669